Available online at www.sciencedirect.com

ScienceDirect

www.elsevier.com/locate/jes

JES JOURNAL OF ENVIRONMENTAL SCIENCES

www.jesc.ac.cn

Evaluation and impact factors of indoor and outdoor gas-phase nitrous acid under different environmental conditions

Yan Chen[1,2], *Weigang Wang*[1,2,*], *Chaofan Lian*[1,2], *Chao Peng*[1,2], *Wenyu Zhang*[1,2], *Junling Li*[1,2], *Mingyuan Liu*[1,2], *Bo Shi*[1,2], *Xuefei Wang*[2,*], *Maofa Ge*[1,2,3]

[1] *State Key Laboratory for Structural Chemistry of Unstable and Stable Species, Beijing National Laboratory for Molecular Sciences (BNLMS), CAS Research/Education Center for Excellence in Molecular Sciences, Institute of Chemistry, Chinese Academy of Sciences, Beijing 100190, China*

[2] *School of Chemical Sciences, University of Chinese Academy of Sciences, Beijing 100049, China*

[3] *Center for Excellence in Regional Atmospheric Environment, Institute of Urban Environment, Chinese Academy of Science, Xiamen 361021, China*

ARTICLE INFO

Article history:
Received 17 May 2019
Revised 30 September 2019
Accepted 17 March 2020
Available online 4 May 2020

Keywords:
Indoor HONO
Indoor pollutants
Heterogeneous reaction
Nitrous acid
Indoor oxidizing capability
Urban area

ABSTRACT

As an important indoor pollutant, nitrous acid (HONO) can contribute to the concentration of indoor OH radicals by photolysis via sunlight penetrating into indoor environments, thus affecting the indoor oxidizing capability. In order to investigate the concentration of indoor HONO and its impact factors, three different indoor environments and two different locations in urban and suburban areas were selected to monitor indoor and outdoor pollutants simultaneously, including HONO, NO, NO_2, nitrogen oxides (NO_x), O_3, and particle mass concentration. In general, the concentration of indoor HONO was higher than that outdoors. In the urban area, indoor HONO with high average concentration (7.10 ppbV) was well-correlated with the temperature. In the suburban area, the concentration of indoor HONO was only about 1-2 ppbV, and had a good correlation with indoor relative humidity. It was mainly attributed to the heterogeneous reaction of NO_2 on indoor surfaces. The sunlight penetrating into indoor environments from outside had a great influence on the concentration of indoor HONO, leading to a concentration of indoor HONO close to that outdoors.

Introduction

A series of reactions in the atmosphere are related to the atmospheric oxidation capacity, in which the OH radical plays an important role (Lelieveld et al., 2008). The photolysis of nitrous acid (HONO) can contribute up to 56% of primary OH radicals throughout the day (Alicke, 2002, 2003; Kleffmann, 2007). Extensive research has been conducted on the sources of HONO (Cui et al., 2018; Huang et al., 2017; Wang et al., 2017), and many reaction mechanisms on the generation of HONO have been proposed. Briefly, the sources of nitrous acid can be roughly divided into two categories. One is direct emission, such as traffic emissions from vehicles (Kirchstetter et al., 1996; Kurtenbach et al., 2001;

* Corresponding authors.
E-mails: wangwg@iccas.ac.cn (W. Wang), wangxf@ucas.ac.cn (X. Wang).

https://doi.org/10.1016/j.jes.2020.03.048
1001-0742/

Liang et al., 2017) and biomass burning (Akagi et al., 2011). The other is secondary reaction processes, which are mainly derived from the homogeneous reaction between OH radicals and NO (Atkinson et al., 2004), dark (Finlayson-Pitts et al., 2003) and light-induced heterogeneous conversion of nitrogen dioxide (Monge et al., 2010) on natural or artificial surfaces (Han et al., 2013), and the photolysis of nitric acid, nitrate (Ye et al., 2016; Zhou et al., 2003, 2011) and ortho-nitrophenol (Bejan et al., 2006). Furthermore, as a medium of heterogeneous reaction, soil can also release HONO (Oswald et al., 2013; Su et al., 2011). However, the predictions of model simulations still show large discrepancies with the results of field observations of the concentration of HONO, and the sources of HONO are still under debate (Lee et al., 2016).

Previous studies on HONO have mainly focused on outdoor environments. Only a few studies have measured the concentration levels of indoor HONO in different environments such as living rooms, classrooms and churches in different countries (Lee et al., 2002; Loupa and Rapsomanikis, 2008; Mendez et al., 2017); moreover, its impact factors have not yet been completely understood (Gligorovski et al., 2018; Zhou et al., 2018). Previous studies have focused on the effect of combustion sources such as gas ranges and stoves on the concentration of indoor HONO. In addition to direct emission from various combustion sources, the reaction of nitrogen dioxide on different surfaces contributes to indoor HONO (Mendez et al., 2017). The result simulated by the Interaction with Chemistry and Aerosols-Indoor (INCA-Indoor) model (Hauglustaine et al., 2004; Mendez et al., 2015) does not match the concentration of indoor HONO well (Mendez et al., 2017). Considering the fact that people spend most of their time in indoor environments, the quality of indoor air affects people's health (Bruce et al., 2000; Gligorovski and Abbatt, 2018; Wells et al., 2017). As an important indoor pollutant (Gligorovski, 2016), HONO can also contribute to indoor OH radicals by photolysis via sunlight penetrating into indoor environments, thus affecting the indoor oxidation capability. Compared to other nitrogen-containing compounds such as NO_2 and HNO_3, HONO has a slower removal rate and stays stable for a longer time in indoor environments (Spicer et al., 1993). Besides, HONO exposure shows adverse effects on the respiratory system and cardiopulmonary function (Jarvis et al., 2005; Rasmussen et al., 1995; Sleiman et al., 2010).

In this study, we measured real-time gas-phase HONO concentrations in indoor and adjacent outdoor areas. In addition, we evaluated the concentration of HONO in different indoor environments and different locations and explored its possible influence factors.

1. Materials and methods

1.1. *Measurement sites*

In order to explore the impact of different outdoor environments on the concentration of indoor HONO, the indoor HONO concentrations of two different locations were investigated.

(1) Urban area. The Institute of Chemistry Chinese Academy of Sciences (ICCAS), which is located in the Haidian District of Beijing, is close to North Ring 4 with heavy traffic and represents a typical urban area with heavy pollution. The laboratory is on the first floor of building No. 2 of ICCAS. It is 6.5 meters long, 5.6 meters wide and 3 meters high with part of the space occupied by several gas analyzers and a Dual-Reactor Chamber (Wang et al., 2015) for simulating atmospheric reactions. The windows of the laboratory face north and there was almost no sunlight shining in during the measurement period. The indoor and outdoor relative solar spectral irradiance at noon are shown in Appendix A Fig. S1. All the points where light intensity was measured indoors were close to the windows (Kahan, 2018; Kleffmann, 2018). The observation was conducted from July 29 to August 9, 2017. Two sets of instruments were deployed in the laboratory to monitor the changes of pollutants, including indoor and outdoor HONO. The temperature in the room was controlled at 25°C by an air conditioner. The sampling line of instruments for outdoor observation passed through the wall of the laboratory, and was 3 m above the ground. The total length of sampling line was as short as possible to minimize the influence of the tube. As to the indoor environment, HONO, nitrogen oxides (NO_x) ($NO+NO_2$), O_3, particle mass concentration, temperature (*T*), and relative humidity (RH) were measured. Similarly, HONO, NO_x, O_3, particle mass concentration, *T*, and RH in the outdoor environment were also measured simultaneously by another set of instruments.

(2) Suburban area. The Lake Yanqi campus of University of Chinese Academy of Sciences (UCAS) is located in Huairou District, 60 km away from the main urban area of Beijing, with lighter pollution. The air conditions at this place have been studied many times previously (Li et al., 2017). We selected a classroom and a laboratory as observation sites. For the classroom, we chose one with 150 seats, 13.7 meters long, 10 meters wide and 3.3 meters high. Its windows faced north, and there was almost no direct sunlight exposure. The indoor and outdoor relative solar spectral irradiance at noon are shown in Appendix A Fig. S2. The indoor and outdoor HONO, RH and *T* were measured on October 1, 2017. In addition, the concentrations of indoor O_3 and NO_x were measured by an ozone analyzer and a NO_x analyzer, respectively. Unfortunately, the NO_x data were lost due to the failure of the NO_x analyzer during observation in the classroom. Similar to the classroom, a laboratory located in Laboratory Building No. 3 with some instruments for physical chemistry teaching was selected as an observation site. It is 6 meters long, 8.8 meters wide and 3.2 meters high. Its windows face south. The indoor and outdoor HONO, RH and *T* were observed on September 26-28 and October 26-29, 2017. During the period from 26 to 28 in September, 2017, the curtains of windows of the laboratory were completely shut, so the sunlight from outside could not enter the room. The intensity of light in the room was weak, and the indoor and outdoor relative solar spectral irradiance at noon are shown in Appendix A Fig. S3. During the period from 26 to 29 in October, 2017, the curtains on the windows of the laboratory were completely opened, and the indoor and outdoor relative solar spectral irradiance at noon are shown in Appendix A Fig. S4. In addition, the concentrations of indoor O_3 and NO_x were measured. It should be noted that during observation, neither the classroom nor the laboratory were in use.

Observation parameters are listed in Table 1. None of these observation sites had combustion sources, such as gas range or stoves. All air conditioners were only used to adjust indoor temperature, not for air exchange. The doors and windows of all observation sites were closed and there was no ventilation, thus the air exchange rate (AER) between the indoor and outdoor environments could be considered to be zero.

1.2. *Measurement instruments*

1.2.1. *Measurement instrument for HONO*

Indoor and outdoor HONO concentrations were observed by two sets of WLPAP (water-based long path absorption photometer). Briefly, ambient HONO was absorbed by deionized water ($\geq$ 18.2 MΩ·cm, DURA, USA) in a two-channel stripping coil. In the first coil, almost all of the HONO and a small

Table 1 – Measurement sites and corresponding observation parameters.

Area	Location	Sites	Dimensions	Orientation of windows	Date	Observation parameters	
						Indoor	Outdoor
Urban	ICCAS	Laboratory	6.5 m long, 5.6 m wide, 3 m high	North	July 29 to August 9, 2017	HONO, NO_x, O_3, mass concentration, RH, *T*	HONO, NO_x, O_3, mass concentration, RH, *T*
Suburban	Lake Yanqi campus of UCAS	Classroom	13.7m long, 10 m wide, 3.3 m high	North	October 1, 2017	HONO, O_3, RH, *T*	HONO, RH, *T*
		Laboratory	6 m long, 8.8 m wide, 3.2 m high	South	September 26-28 and October 26-29, 2017	HONO, NO_x, O_3, RH, *T*	HONO, RH, *T*

ICCAS: Institute of Chemistry Chinese Academy of Sciences; UCAS: University of Chinese Academy of Sciences.

fraction of known interfering species (e.g., NO_2, SO_2, peroxyacetyl nitrate) were absorbed; while in the second channel, only a small fraction of known interfering species was absorbed. The solution after absorption was then mixed with a solution of 2 mmol/L sulfanilamide, 77 μmol/L *n*-(1-naphthyl)-ethylenediamine dihydrochloride and 144 mmol/L hydrogen chloride to form the azo dye derivative. The derivative was pumped into a LWCC (liquid waveguide capillary cell, LWCC-3250, WPI, USA) and was quantified by light absorbance at 550 nm using a fiber optic spectrometer (USB4000, OceanOptics, USA). The gas pumping speed was controlled by a flowmeter (CS200, Sevenstar, China) with an aspirator pump (N811KTDC, KNF, Germany) set to 1 L/min. The liquid flow rate was controlled by the rotation speed of the peristaltic pump (MT12, Easypump, China), set to 0.5 mL/min. Since any small bubble in the solution would greatly affect the light signals, a debubbler (bubble trap for microfluidics kit, Elveflow, France) was added before the LWCC. The WLPAP has a detection limit of 5 pptV with a time response of 7 min. The HONO analyzer was calibrated by zero air every 24 hours to check whether it was in normal operation. It was also calibrated by a nitrite standard solution before and after every measurement. We adjusted the time forward by 7 min in the data processing of HONO based on the time response.

As the commercial LOPAP (long path absorption photometer) used a highly acidic solution to absorb ambient HONO, it raised the risk of acid corrosion to the instrument (Heland et al., 2001). Since deionized water had been proved to efficiently absorb ambient HONO via a stripping coil (Huang et al., 2002; Zhou et al., 2011; Xue et al., 2019), using deionized water would be much more convenient. The two-channel principle was based on the known interfering species having a rather low solubility in water, so the real HONO concentration was defined by the concentration in the first channel minus that in the second channel. To carry out a further evaluation of WLPAP, a comparison observation was conducted with a home-made LOPAP which had been proved to work well in field and laboratory measurements (Zhou et al., 2015; Hou et al., 2016; Xue et al., 2019). There were both indoor and outdoor comparisons in the observation. Both the results indicated good correlation. As shown in Appendix A Fig. S5a, the WLPAP and home-made LOPAP showed good agreement for the absolute concentration and the variation trend. The correlation of the two HONO concentrations (slope = 0.96754, R^2 = 0.99741) indicated the satisfactory performance of WLPAP.

1.2.2. *Measurement instruments for other parameters*

During the observation, all parameters except HONO were measured by commercially available instruments. For the urban area, indoor pollutants including NO_x, O_3, and particle mass concentration were measured by a commercial NO_x analyzer (T200UP, API, USA), O_3 analyzer (T400, API, USA) and scanning mobility particle sizer (SMPS), which consisted of an electrostatic classifier (EC 3080, TSI, USA), differential mobility analyzer (DMA 3081, TSI, USA) and condensation particle counter (CPC 3772, TSI, USA). Meanwhile, the outdoor NO_x, O_3, and particle mass concentrations were measured by a commercial NO_x analyzer (T200, API, USA), O_3 analyzer (49i, Thermo, USA) and SMPS (EC 3080, DMA 3081, CPC 3776, TSI, USA). The indoor and outdoor temperature and relative humidity were measured by two sets of relative humidity and temperature probes (HMP110, VAISALA, Finland). Both sets of observation instruments were calibrated before and after measurement.

For the suburban area, limited by the observation site conditions, only one set of instruments was available. Compared with outdoors, we focused on the concentrations of indoor pollutants. The concentrations of NO_x and O_3 in the classroom and laboratory were measured by a commercial NO_x analyzer (T200, API, USA) and O_3 analyzer (49i, API, USA). The indoor and outdoor temperature and relative humidity were measured by two sets of relative humidity and temperature probes (HMP110, VAISALA, Finland). As to indoor and outdoor HONO, since the interference in the second channel was negligible during the observation, we changed the two channels into the parallel state. The first channel was used for indoor measurement, and the second channel was used for outdoor measurement.

2. Results and discussion

2.1. *Time series of indoor and outdoor observation parameters*

For the urban area, Fig. 1 shows the time series of indoor and outdoor concentrations of NO, NO_2, NO_x, O_3 and particle mass concentration in the laboratory of ICCAS during the observation period. It can be seen that there was a partial loss of data for outdoor O_3 due to the failure of the computer used for data collection. Fig. 2 shows the time series of indoor and outdoor RH and *T* in the laboratory of ICCAS. Average concentrations of relevant species and corresponding indoor-to-outdoor ratios are listed in Table 2. As shown in Fig. 2 and Table 2, the average concentration of indoor HONO was 7.10 ppbV, and the average concentration of outdoor HONO was only 0.72 ppbV. The concentration of indoor HONO was about ten times higher than that outdoors. As to NO, NO_2, and NO_x, the concentrations of indoor pollutants were also higher than those out-

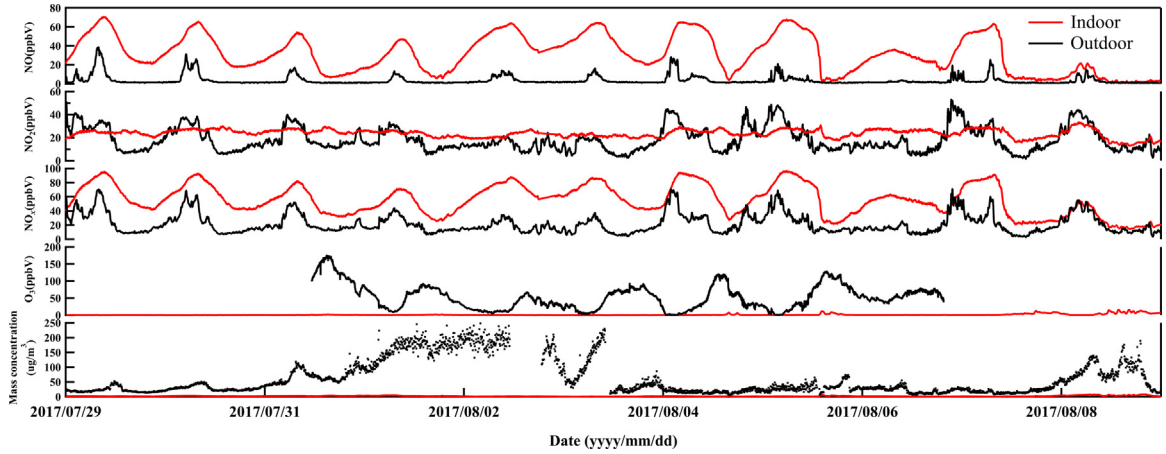

Fig. 1 – Time series of indoor and outdoor NO, NO_2, nitrogen oxides (NO_x), mass concentration and O_3 at 15-min average in the laboratory of ICCAS during the observation period from July 29 to August 9, 2017.

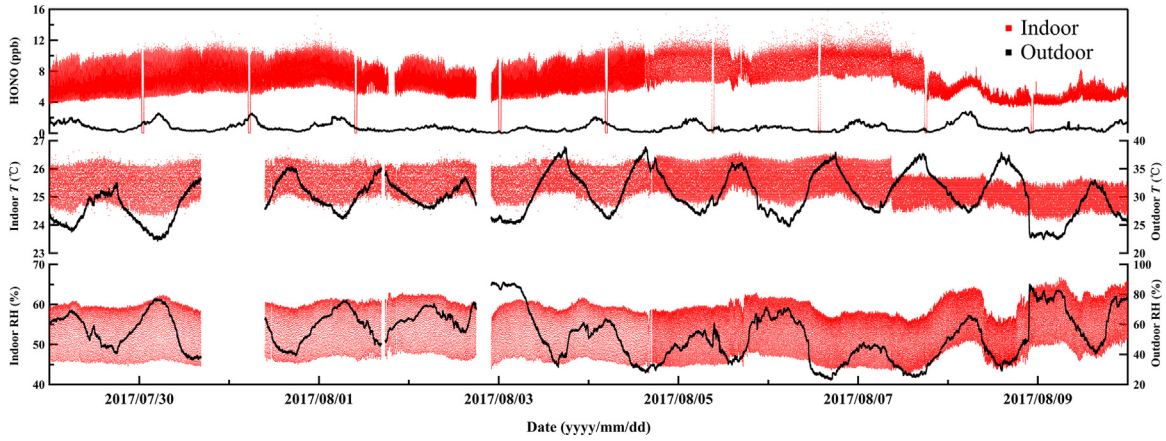

Fig. 2 – Time series of indoor and outdoor HONO, relative humidity (RH), and temperature (T) in the laboratory of ICCAS during the observation period from July 29 to August 9, 2017.

Table 2 – Average concentrations of relevant species and corresponding indoor-to-outdoor ratios in the laboratory of ICCAS during the observation period from July 29 to August 9, 2017.

Pollutants	Average concentration		Indoor/Outdoor
	Indoor	Outdoor	
HONO (ppbV)	7.10	0.72	9.9
NO (ppbV)	29.45	3.50	8.4
NO_2 (ppbV)	23.28	17.90	1.3
NO_x (ppbV)	52.73	21.40	2.5
O_3 (ppbV)	1.89	52.85	0.036
Mass concentration ($\mu g/m^3$)	2.54	61.80	0.041

doors. However, the O_3 and particle mass concentrations were much lower than outdoors. Since there was no ventilation in the laboratory and it was closed, there was no clear correlation between indoor HONO and outdoor HONO, and they showed different patterns of diurnal variation. The outdoor HONO exhibited a typical character such that it was low in the daytime and high at night. The indoor HONO showed periodic changes, and its period was about 15 minutes. Fig. 2 shows that the outdoor temperature and relative humidity exhibited a normal inverse relationship, and when the temperature was high, the relative humidity was low and vice versa. However, the indoor temperature and relative humidity also exhibited periodic changes and the 15-minute period was the same as that of indoor HONO.

For the suburban area, time series of indoor and outdoor HONO, NO, NO_2, NO_x, O_3 in the classroom and laboratory of UCAS are shown in Appendix A Figs. S6-S8. The concentration of indoor HONO was much lower when the concentration of outdoor HONO was at a low level. As to indoor temperature and relative humidity, no periodic changes were observed.

2.2. *Impact factors on indoor HONO*

2.2.1. *Temperature*

As to the observation in the laboratory of ICCAS, we found that the indoor temperature and relative humidity exhibited periodic changes under the influence of the air conditioner, while indoor HONO also exhibited the same periodic changes. It should be emphasized that the air conditioner was only used to adjust indoor temperature, not for air exchange. In order to confirm the role of the air conditioner, we turned

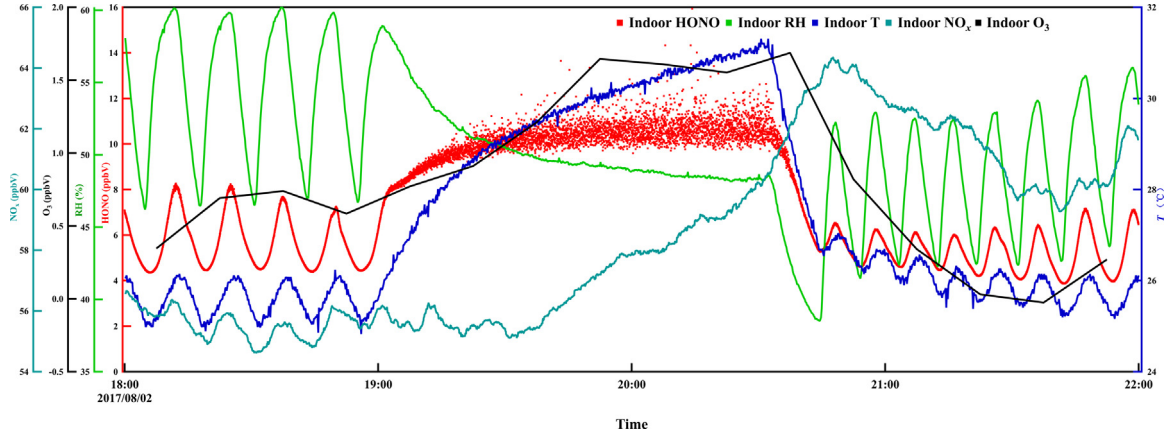

Fig. 3 – Temporal variations of indoor HONO, NO_x, O_3, RH, and *T* during the period when the air conditioner was turned off in the laboratory of ICCAS.

it off during the observation period to monitor the changes of relevant observation parameters. The air conditioner was off from 7:00 pm to 8:30 pm on August 2, 2017. At this time, it was raining outside, so the indoor temperature did not increase too much. Fig. 3 shows the temporal variations of indoor HONO, NO_x, O_3, RH, and *T* during the period when the air conditioner was turned off. As the air conditioner turned off, the indoor temperature rose and the relative humidity decreased. They showed a normal reverse correlation and neither of them showed periodic variations. For indoor HONO, periodic changes were no longer observed and the concentration increased with indoor temperature to a stable state. When the air conditioner was turned off and the indoor temperature increased, the indoor NO_x also increased but there was a time lag, and the indoor O_3, with low concentration, also increased. When the air conditioner was turned on again, the temperature decreased and indoor relative humidity increased, and periodic changes resumed, including for the HONO concentration. Indoor NO_x and O_3 showed a downward trend and indoor NO_x still had a time lag. According to the changes of indoor-related observation parameters, we identified that the air conditioner controlled the indoor temperature and relative humidity and then affected the changes of the indoor observation parameters, especially the real-time concentration of indoor HONO. It is reasonable to postulate that indoor HONO adsorbed and desorbed on indoor surfaces (Kim and Kang, 2010). As shown in Fig. 1, the O_3 and particle mass concentrations were much lower than outdoors. The indoor-to-outdoor ratios of O_3 and particle mass concentration were close to zero. The indoor surfaces are likely an efficient sink for O_3. The conversion from NO to NO_2 is inefficient in this situation. On the other hand, the high indoor concentration of HONO in the urban area may be another source of NO in the lab. The concentration of NO in the outdoor environment is also high during the night because the observation site is not far from the main road, and emission from vehicles may be another source of NO to the indoor environment.

As to the observation in UCAS, we did not observe a periodic variation of indoor temperature and humidity. This may be due to the difference between indoor and outdoor temperatures under a different external environment.

2.2.2. *Correlation of indoor and outdoor HONO with NO, NO_2, O_3, particle mass concentration, RH, and T*

In order to investigate the source of indoor HONO, correlation analysis with other relevant observation parameters such as

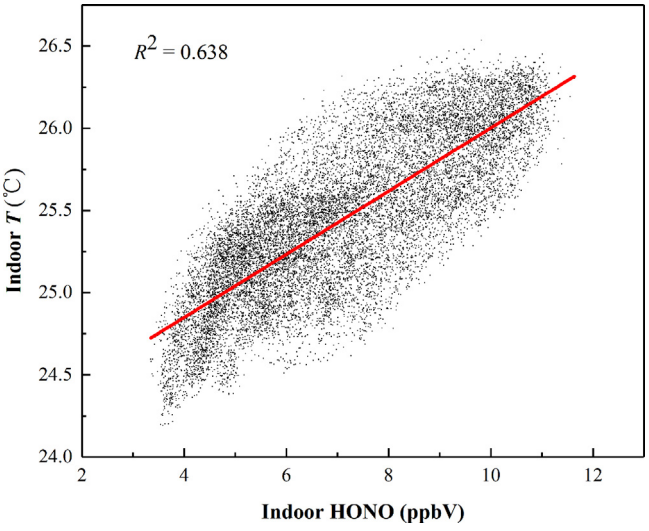

Fig. 4 – Association between indoor HONO and indoor *T* at 1-min average in the laboratory of ICCAS during the observation period from July 29 to August 9, 2017.

NO, NO_2, NO_x, O_3, particle mass concentration, RH, and *T* was conducted. For the outdoor HONO, the same correlation studies were also conducted. The results of the correlation studies are listed in Appendix A Tables S1-S2. Similarly, for the data observed in the classroom and laboratory of UCAS, the correlation between indoor HONO and outdoor HONO and other observation parameters was also studied. The results of the correlation studies are listed in Appendix A Tables S3-S8.

Correlation analysis was also performed based on the urban data, and we found that indoor HONO was strongly related to temperature when the concentration indoors was high. In the urban area, indoor HONO changed with indoor temperature and showed a good correlation. Indoor HONO adsorbed onto and desorbed from surfaces when the average concentration of indoor HONO was high, at a level of 7.10 ppbV. The correlation between indoor HONO and indoor *T* in the laboratory of ICCAS is shown in Fig. 4. The results of the correlation analysis were also consistent with the experiment carried out with the air conditioner off as described above. For the other correlation data, the indoor NO accounted for most of the indoor NO_x, so a correlation of 0.979 was observed between them. The

Table 3 – Average concentrations of relevant species and corresponding indoor-to-outdoor ratios in the classroom and laboratory of UCAS.

Sites	Location		Average concentration					Indoor HONO/Indoor NO_2	Indoor HONO/Outdoor HONO
			Indoor HONO	Indoor NO	Indoor NO_2	Indoor O_3	Outdoor HONO		
Lake Yanqi campus of UCAS	Classroom		1.68	-	-	5.4	0.75	-	2.24
	Laboratory	Curtains shut	1.91	9.9	8.2	4.8	0.59	0.23	3.24
		Curtains open	1.05	7.7	9.4	8.9	0.98	0.11	1.07

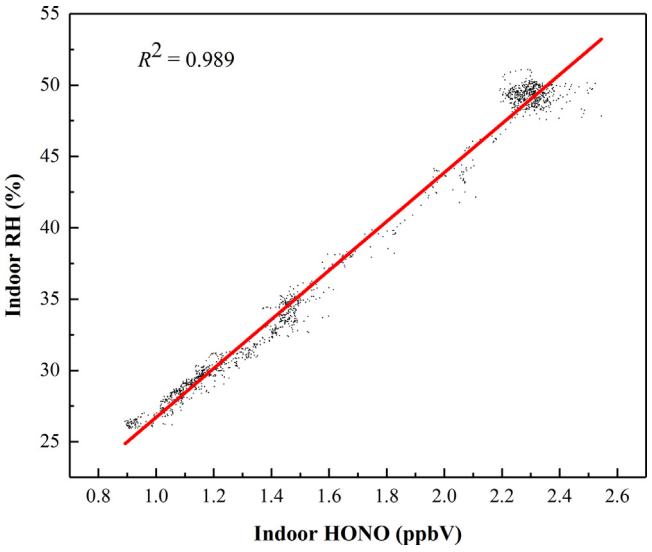

Fig. 5 – Association between indoor HONO and indoor RH at 1-min average in the classroom of UCAS on the day of the National Day in the year of 2017.

concentration of indoor O_3 was at a very low level because of the high concentration of indoor NO during the observation period. There was a negative correlation between indoor O_3 and indoor NO. The indoor particle mass concentration was at a very low level, and the correlation with other parameters was not high, especially the indoor HONO. Here, the surface area of the particles is negligible in comparison to that of indoor surfaces. For the outdoor correlation, compared with indoor HONO, the correlation between outdoor HONO and NO_2 was higher, reaching 0.670. The concentration of indoor HONO is higher than outdoors when their NO_2 levels are similar. However, the correlation between HONO and temperature outdoors is not significant. In addition, outdoor NO_x was dominated by NO_2 rather than NO, so the correlation between NO_2 and NO_x was excellent, reaching 0.921. The anti-correlation between outdoor O_3 and outdoor NO_x was the same as that indoors. Different from indoors, the outdoor temperature and relative humidity showed normal anti-correlation. Normally, NO_2 has been considered the main precursor of HONO. The source of indoor HONO could be generation during the heterogeneous reaction of NO_2 on various surfaces. The indoor HONO/NO_2 in the urban area showed a good correlation with indoor *T* (Appendix A Fig. S10), but a lack of correlation with indoor RH (Appendix A Fig. S9). It is reasonable to postulate that indoor HONO adsorbed and desorbed on indoor surfaces, influenced by temperature.

Furthermore, the correlation between indoor HONO and indoor *T* was not good in the suburban area. The adsorption and desorption of indoor HONO on indoor surfaces was not obvious when HONO was at a lower level. The indoor HONO concentration was highly correlated with the indoor RH, reaching 0.989, indicating that the source of indoor HONO should be the heterogeneous reaction of NO_2 on various surfaces (Finlayson-Pitts et al., 2003; Gandolfo et al., 2017). The correlation between indoor HONO and indoor RH in the classroom of UCAS is shown in Fig. 5.

2.2.3. *Effect of sunlight on indoor HONO*

Only the windows of the laboratory in UCAS faced south, while the other windows faced north (Table 1). During the observation, we found that the orientation of windows, i.e. the sunlight, has a great influence on the concentration of indoor HONO and the indoor-to-outdoor ratio of HONO. Indoor HONO may decompose into OH radicals by photolysis initiated by sunlight (less than 390 nm), which is an important removal pathway for indoor HONO (Gomez Alvarez et al., 2013). Average concentrations of relevant species and corresponding indoor-to-outdoor ratios are listed in Table 3. Comparing the data of the laboratory under different conditions, the difference between curtains shut and curtains open can be seen. When allowing sunlight to enter into room, the concentrations of indoor and outdoor HONO were close and the indoor-to-outdoor ratio of HONO was only 1.07. When sunlight was blocked, the ratio was up to 3.24. Meanwhile, the efficiency of NO_2 converting to HONO was also higher, and the ratio of indoor HONO to indoor NO_2 also rose from 0.11 to 0.23.

3. Conclusions

In the present work, indoor and outdoor concentrations of HONO in both urban and suburban areas were investigated. The results show that the indoor concentration was higher than that outdoors. In the urban area, the concentration of indoor HONO changed with indoor temperature and showed good positive correlation, reaching 0.638. Indoor HONO may be adsorbed on surfaces when the average concentration of indoor HONO is over 7.10 ppbV and desorb when it decreases to lower than this value. In the suburban area, the average concentration of indoor HONO was relatively low, at a level of 1-2 ppbV. Indoor HONO had good correlation with the humidity, reaching 0.989. The heterogeneous reaction of NO_2 on indoor surfaces may contribute to indoor HONO. The sunlight shining into a room from outside may lead to the indoor concentration decreasing and becoming close to that outside, which could be ascribed to the photolysis to NO_x. Thus, the ratio of indoor HONO to NO_2 decreased under sunlight. Further studies on other impact factors affecting the concentration of indoor HONO and the source of indoor HONO remain to be elucidated in future work.

Acknowledgments

This project was supported by The National Key Research and Development Program of China (No. 2017YFC0209500), National research program for key issues in air pollution control (No. DQGG-0103), and the National Natural Science Foundation of China (Nos. 41822703 and 91744204).

Appendix A. Supplementary data

Supplementary material associated with this article can be found in the online version at doi:10.1016/j.jes.2020.03.048.

REFERENCES

Akagi, S.K., Yokelson, R.J., Wiedinmyer, C., Alvarado, M.J., Reid, J.S., Karl, T., et al., 2011. Emission factors for open and domestic biomass burning for use in atmospheric models. Atmos. Chem. Phys. 11, 4039–4072.

Alicke, B., 2002. Impact of nitrous acid photolysis on the total hydroxyl radical budget during the Limitation of Oxidant Production/Pianura Padana Produzione di Ozono study in Milan. J. Geophys. Res. 107 (D22) LOP 9-1-LOP 9-17.

Alicke, B., 2003. OH formation by HONO photolysis during the BERLIOZ experiment. J. Geophys. Res. 108 (D4) PHO 3-1-PHO 3-17.

Atkinson, R., Baulch, D.L., Cox, R.A., Crowley, J.N., Hampson, R.F., Hynes, R.G., et al., 2004. Evaluated kinetic and photochemical data for atmospheric chemistry: Volume I - gas phase reactions of O_x, HO_x, NO_x and SO_x species. Atmos. Chem. Phys. 4, 1461–1738.

Bejan, I., Abd-el-Aal, Y., Barnes, I., Benter, T., Bohn, B., Wiesen, P., et al., 2006. The photolysis of ortho-nitrophenols: a new gas phase source of HONO. Phys. Chem. Chem. Phys. 8, 2028–2035.

Bruce, N., Perez-Padilla, R., Albalak, R., 2000. Indoor air pollution in developing countries: a major environmental and public health challenge. Bull. World Health Organ. 78, 1078–1092.

Cui, L., Li, R., Zhang, Y., Meng, Y., Fu, H., Chen, J., 2018. An observational study of nitrous acid (HONO) in Shanghai, China: The aerosol impact on HONO formation during the haze episodes. Sci. Total Environ. 630, 1057–1070.

Finlayson-Pitts, B.J., Wingen, L.M., Sumner, A.L., Syomin, D., Ramazan, K.A., 2003. The heterogeneous hydrolysis of NO_2 in laboratory systems and in outdoor and indoor atmospheres: An integrated mechanism. Phys. Chem. Chem. Phys. 5, 223–242.

Gandolfo, A., Rouyer, L., Wortham, H., Gligorovski, S., 2017. The influence of wall temperature on NO_2 removal and HONO levels released by indoor photocatalytic paints. Appl. Catal. B 209, 429–436.

Gligorovski, S., 2016. Nitrous acid (HONO): An emerging indoor pollutant. J. Photochem. Photobiol. A 314, 1–5.

Gligorovski, S., Abbatt, J.P.D., 2018. An indoor chemical cocktail. Science 359, 631–632.

Gligorovski, S., Li, X., Herrmann, H., 2018. Indoor (photo)chemistry in China and resulting health effects. Environ. Sci. Technol. 52, 10909–10910.

Gomez Alvarez, E., Amedro, D., Afif, C., Gligorovski, S., Schoemaecker, C., Fittschen, C., et al., 2013. Unexpectedly high indoor hydroxyl radical concentrations associated with nitrous acid. Proc. Natl. Acad. Sci. USA 110, 13294–13299.

Han, C., Liu, Y., He, H., 2013. Heterogeneous photochemical aging of soot by NO_2 under simulated sunlight. Atmos. Environ. 64, 270–276.

Hauglustaine, D.A., Hourdin, F., Jourdain, L., Filiberti, M.A., Walters, S., Lamarque, J.F., et al., 2004. Interactive chemistry in the Laboratoire de Meteorologie Dynamique general circulation model: Description and background tropospheric chemistry evaluation. J. Geophys. Res.-Atmos. 109, 55.

Heland, J., Kleffmann, J., Kurtenbach, R., Wiesen, P., 2001. A new instrument to measure gaseous nitrous acid (HONO) in the atmosphere. Environ. Sci. Technol. 35, 3207–3212.

Hou, S., Tong, S., Ge, M., An, J., 2016. Comparison of atmospheric nitrous acid during severe haze and clean periods in Beijing, China. Atmos. Environ. 124 (Part B), 199–206.

Huang, G., Zhou, X., Deng, G., Qiao, H., Civerolo, K., 2002. Measurements of atmospheric nitrous acid and nitric acid. Atmos. Environ. 36, 2225–2235.

Huang, R.-J., Yang, L., Cao, J., Wang, Q., Tie, X., Ho, K.-F., et al., 2017. Concentration and sources of atmospheric nitrous acid (HONO) at an urban site in Western China. Sci. Total Environ. 593-594, 165–172.

Jarvis, D.L., Leaderer, B.P., Chinn, S., Burney, P.G., 2005. Indoor nitrous acid and respiratory symptoms and lung function in adults. Thorax 60, 474–479.

Kahan, T.F., 2018. Response to Comment on "Wavelength-resolved photon fluxes of indoor light sources: Implications for HO_x production". Environ. Sci. Technol. 52, 11966–11967.

Kim, S.K., Kang, H., 2010. Efficient conversion of nitrogen dioxide into nitrous acid on ice surfaces. J. Phys. Chem. Lett. 1, 3085–3089.

Kirchstetter, T.W., Harley, R.A., Littlejohn, D., 1996. Measurement of nitrous acid in motor vehicle exhaust. Environ. Sci. Technol. 30, 2843–2849.

Kleffmann, J., 2007. Daytime sources of nitrous acid (HONO) in the atmospheric boundary layer. ChemPhysChem 8, 1137–1144.

Kleffmann, J., 2018. Comment on "Wavelength-resolved photon fluxes of indoor light sources: Implications for HO_x production". Environ. Sci. Technol. 52, 11964–11965.

Kurtenbach, R., Becker, K.H., Gomes, J.A.G., Kleffmann, J., Lorzer, J.C., Spittler, M., et al., 2001. Investigations of emissions and heterogeneous formation of HONO in a road traffic tunnel. Atmos. Environ. 35, 3385–3394.

Lee, J.D., Whalley, L.K., Heard, D.E., Stone, D., Dunmore, R.E., Hamilton, J.F., et al., 2016. Detailed budget analysis of HONO in central London reveals a missing daytime source. Atmos. Chem. Phys. 16, 2747–2764.

Lee, K., Xue, X.P., Geyh, A.S., Ozkaynak, H., Leaderer, B.P., Weschler, C.J., et al., 2002. Nitrous acid, nitrogen dioxide, and ozone concentrations in residential environments. Environ. Health Perspect. 110, 145–149.

Lelieveld, J., Butler, T.M., Crowley, J.N., Dillon, T.J., Fischer, H., Ganzeveld, L., et al., 2008. Atmospheric oxidation capacity sustained by a tropical forest. Nature 452, 737–740.

Li, K., Li, J.L., Wang, W.G., Tong, S.R., Liggio, J., Ge, M.F., 2017. Evaluating the effectiveness of joint emission control policies on the reduction. of ambient VOCs: Implications from observation during the 2014 APEC summit in suburban Beijing. Atmos. Environ. 164, 117–127.

Liang, Y., Zha, Q., Wang, W., Cui, L., Lui, K.H., Ho, K.F., et al., 2017. Revisiting nitrous acid (HONO) emission from on-road vehicles: A tunnel study with a mixed fleet. J. Air Waste Manage. Assoc. 67, 797–805.

Loupa, G., Rapsomanikis, S., 2008. Air pollutant emission rates and concentrations in medieval churches. J. Atmos. Chem. 60, 169–187.

Mendez, M., Blond, N., Amedro, D., Hauglustaine, D.A., Blondeau, P., Afif, C., et al., 2017. Assessment of indoor HONO formation mechanisms based on in situ measurements and modeling. Indoor Air 27, 443–451.

Mendez, M., Blond, N., Blondeau, P., Schoemaecker, C., Hauglustaine, D.A., 2015. Assessment of the impact of oxidation processes on indoor air pollution using the new time-resolved INCA-Indoor model. Atmos. Environ. 122, 521–530.

Monge, M.E., D'Anna, B., Mazri, L., Giroir-Fendler, A., Ammann, M., Donaldson, D.J., et al., 2010. Light changes the atmospheric reactivity of soot. Proc. Natl. Acad. Sci. USA 107, 6605–6609.

Oswald, R., Behrendt, T., Ermel, M., Wu, D., Su, H., Cheng, Y., et al., 2013. HONO emissions from soil bacteria as a major source of atmospheric reactive nitrogen. Science 341, 1233–1235.

Rasmussen, T.R., Brauer, M., Kjaergaard, S., 1995. Effects of nitrous-acid exposure on human mucous-membranes. Am. J. Respir. Crit. Care Med. 151, 1504–1511.

Sleiman, M., Gundel, L.A., Pankow, J.F., Jacob III, P., Singer, B.C., Destaillats, H., 2010. Formation of carcinogens indoors by surface-mediated reactions of nicotine with nitrous acid, leading to potential thirdhand smoke hazards. Proc. Natl. Acad. Sci. USA 107, 6576–6581.

Spicer, C.W., Kenny, D.V., Ward, G.F., Billick, I.H., 1993. Transformations, lifetimes, and sources of NO_2, HONO, and HNO_3 in indoor environments. J. Air Waste Manage. Assoc. 43, 1479–1485.

Su, H., Cheng, Y.F., Oswald, R., Behrendt, T., Trebs, I., Meixner, F.X., et al., 2011. Soil nitrite as a source of atmospheric HONO and OH radicals. Science 333, 1616–1618.

Wang, J.Q., Zhang, X.S., Guo, J., Wang, Z.W., Zhang, M.G., 2017. Observation of nitrous acid (HONO) in Beijing, China: Seasonal variation, nocturnal formation and daytime budget. Sci. Total Environ. 587, 350–359.

Wang, W.-G., Li, K., Zhou, L., Ge, M.-F., Hou, S.-Q., Tong, S.-R., et al., 2015. Evaluation and application of dual-reactor chamber for studying atmospheric oxidation processes and mechanisms. Acta Phys. Chim. Sin. 31, 1251–1259.

Wells, J.R., Schoemaecker, C., Carslaw, N., Waring, M.S., Ham, J.E., Nelissen, I., et al., 2017. Reactive indoor air chemistry and health-A workshop summary. Int. J. Hyg. Environ. Health. 220, 1222–1229.

Xue, C., Ye, C., Ma, Z., Liu, P., Zhang, Y., Zhang, C., et al., 2019. Development of stripping coil-ion chromatograph method and intercomparison with CEAS and LOPAP to measure atmospheric HONO. Sci. Total Environ. 646, 187–195.

Ye, C., Zhou, X., Pu, D., Stutz, J., Festa, J., Spolaor, M., et al., 2016. Rapid cycling of reactive nitrogen in the marine boundary layer. Nature 532, 489–491.

Zhou, L., Wang, W., Hou, S., Tong, S., Ge, M., 2015. Heterogeneous uptake of nitrogen dioxide on Chinese mineral dust. J. Environ. Sci. 38, 110–118.

Zhou, S., Young, C.J., VandenBoer, T.C., Kowal, S.F., Kahan, T.F., 2018. Time-resolved measurements of nitric oxide, nitrogen dioxide, and nitrous acid in an occupied New York home. Environ. Sci. Technol. 52, 8355–8364.

Zhou, X.L., Gao, H.L., He, Y., Huang, G., Bertman, S.B., Civerolo, K., et al., 2003. Nitric acid photolysis on surfaces in low-NOx environments: Significant atmospheric implications. Geophys. Res. Lett. 30 (23) ASC 12-1–ASC 12-4.

Zhou, X.L., Zhang, N., TerAvest, M., Tang, D., Hou, J., Bertman, S., et al., 2011. Nitric acid photolysis on forest canopy surface as a source for tropospheric nitrous acid. Nat. Geosci. 4, 440–443.